AIP | Review of Scientific Instruments

Superconducting coplanar waveguide resonators for low temperature pulsed electron spin resonance spectroscopy

H. Malissa, D. I. Schuster, A. M. Tyryshkin, A. A. Houck, and S. A. Lyon

Citation: Review of Scientific Instruments **84**, 025116 (2013); doi: 10.1063/1.4792205
View online: http://dx.doi.org/10.1063/1.4792205
View Table of Contents: http://scitation.aip.org/content/aip/journal/rsi/84/2?ver=pdfcov
Published by the AIP Publishing

Superconducting coplanar waveguide resonators for low temperature pulsed electron spin resonance spectroscopy

H. Malissa,[1,a)] D. I. Schuster,[2] A. M. Tyryshkin,[1] A. A. Houck,[1] and S. A. Lyon[1]
[1]*Department of Electrical Engineering, Princeton University, Olden Street, Princeton, New Jersey 08544, USA*
[2]*Department of Physics and James Franck Institute, University of Chicago, Chicago, Illinois 60637, USA*

(Received 2 January 2013; accepted 29 January 2013; published online 26 February 2013)

We discuss the design and implementation of thin film superconducting coplanar waveguide micro-resonators for pulsed electron spin resonance experiments. The performance of the resonators with P doped Si epilayer samples is compared to waveguide resonators under equivalent conditions. The high achievable filling factor even for small sized samples and the relatively high Q-factor result in a sensitivity of 4.5×10^8 spins per shot, which is superior to that of conventional waveguide resonators, in particular to spins close to the sample surface. The peak microwave power is on the order of a few milliwatts, which is compatible with measurements at ultra-low temperatures. We also discuss the effect of the nonuniform microwave magnetic field on the Hahn echo power dependence.
 [http://dx.doi.org/10.1063/1.4792205]

I. INTRODUCTION

Planar micro-resonators have been demonstrated to be an attractive alternative to conventional waveguide resonators for electron spin resonance (ESR) spectroscopy in situations where the sample volume and therefore the number of spins are small.[1–7] The frequency of transmission line based micro-resonators is determined only by their length along the direction of propagation, whereas both perpendicular dimensions are much shorter than the wavelength. The resonator volume can thus be tailored to be close to the sample volume. Here, we report the design and fabrication of superconducting coplanar waveguides (CPW) resonators for pulsed ESR measurements. The superconducting metallization layer is made to be thin enough to support the static magnetic field required for ESR at 10 GHz. The performance of the devices is demonstrated with spin echo measurements on an isotopically purified ^{28}Si:P.

In contrast to waveguide resonators which are optimized to exhibit a very uniform microwave magnetic field B_1 across the sample volume, the mode pattern of planar micro-resonators is determined by the geometry of the resonator and the planar waveguide. B_1 can therefore be quite inhomogeneous across the sample volume, which make the resonators particularly sensitive to spins close to the surface. The high conversion efficiency of microwave power to B_1 makes these resonators convenient for low temperature operation where the cooling power is limited and microwave heating must be avoided.

In CPW, the center conductor and the ground planes are on the same side of the substrate and are separated by a gap. The impedance is mostly independent of the substrate thickness, thus allowing the waveguide cross section to be arbitrarily small, which further reduces the resonator volume. The use of superconductors as center conductor and ground plane metallization layer supports the resulting high current densities and allows for much higher quality factors compared to structures with normal conductors. CPW resonators are used in connection with superconducting qubits and continuous wave ESR has been demonstrated. In particular, a hybrid system consisting of a superconducting qubit and a spin system that serves as a memory is feasible.[8–12]

II. EXPERIMENTS

A. Resonator fabrication

The superconducting CPW structures are fabricated in 50 nm Nb films sputtered on 0.5 mm thick sapphire substrates at STAR Cryoelectronics. The thickness of 50 nm is selected to ensure that the CPW remains superconducting in the magnetic fields used for X-band ESR experiments (typically 350 mT at 10 GHz). The theoretical in-plane critical field of these films[2] is 1.5 T at 4.2 K, compared to 200 mT for bulk Nb. The resonators and waveguides are patterned using photolithography followed by etching in a 10:1 SF_6:O_2 plasma in a STS inductively coupled plasma etcher. The devices, with a size of 7×2 mm, consist of eight $\lambda/4$ sections of CPW which are capacitively coupled to a common feedline on one end and shorted to ground on the other end (Fig. 1(a)). The fixed coupling is achieved by a 250μm long L-shaped section of the resonator running in parallel to the feedline at a distance of 20 μm.

The length of the individual resonators varies from 2.8 mm to 3.4 mm, which corresponds to microwave frequencies ranging from 8.75 GHz to 10.5 GHz for the given waveguide geometry and the relative dielectric constant of sapphire ($\epsilon_r = 11.5$). The CPW has a center conductor width of 10 μm and a gap width of 4 μm, much smaller than the wavelength. Near the edge of the chip the waveguide is tapered to a width of 150 μm to facilitate interconnection through wire bonding. The transmission feedline serves only for troubleshooting purposes. In our pulsed ESR experiments, one port of the feedline is connected to the spectrometer and the other is

[a)]Present address: Department of Physics and Astronomy, University of Utah, 115 South 1400 East #201, Salt Lake City, Utah 84112, USA.

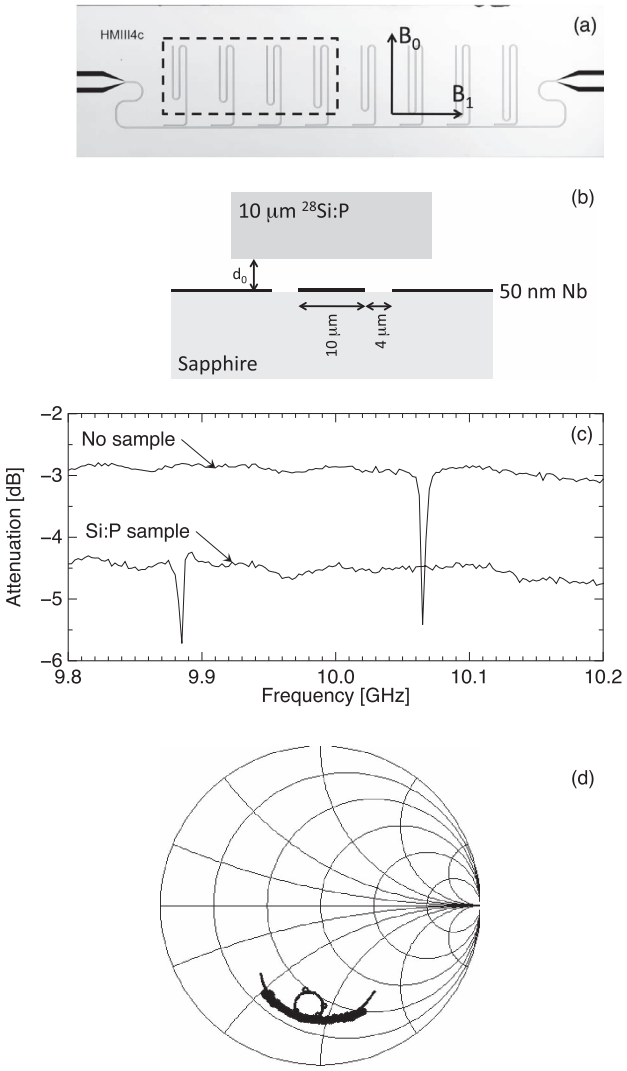

FIG. 1. (a) Photograph of the device, showing eight λ/4 resonators coupled to the common feedline. The Nb film appears gray, and the underlying sapphire substrate is black. The whole device is 7 × 2 mm in size. The dashed rectangle indicates the position where silicon sample was mounted. The arrows indicate the orientation of the external field B_0 and the oscillating field B_1. (b) Cross section of the CPW resonator and the active sample volume. (c) Resonance curves of one of the CPW resonators before and after mounting a silicon sample, measured using a vector network analyzer. The resonance width in both cases is approximately 5 MHz which corresponds to $Q \approx 2000$. (d) Smith Chart plot of the resonance curve (upper trace in (c)).

terminated with a matched load and thus the experiments are done in reflection mode.

B. Test sample

The sample examined is a ∼3 × 1 mm^2 piece of isotopically enriched ^{28}Si:P epilayer of 10 μm thickness with a doping concentration of 1×10^{16}cm^{-3} (indicated as rectangle in Fig. 1(a)). This sample has been investigated intensively in the past, and the decoherence time of $T_2 = 280$ μs and an ESR linewidth of 10 μT were reported[13] for P donors at 7 K. The signal is comparably strong, which makes this sample ideal for demonstration and evaluation purposes.

The sample is flip-chip mounted directly on top of the resonator (see Fig. 1(b)) with the active region of the sample pushed against the CPW as close as possible, with only an air gap in between. The sample was then fixed with a small amount GE varnish as glue. Great care was taken to avoid getting any GE varnish either on top of the CPW or in between sample and resonator that could cause additional losses in the CPW resonator thus lowering its Q. This way, a minimum distance d_0 between sample and resonator surface on the order of a few μm can be achieved.

This mounting scheme results in small uncertainties in the resonator frequency due to the different dielectric constants in the substrate, the sample, and the gap. The integration of several independent resonators with different frequencies on the same device as described above helps to ensure that some of the resonators match the frequency bandwidth of the spectrometer.

The device is oriented such that the external field B_0 is in plane of the device and perpendicular to the microwave B_1 field (see Fig. 1(a)).

C. Characterization

A vector network analyzer (Anritsu MS2028C) is used to characterize the resonators at 4.2 K before and after the sample is mounted (traces are shown in Fig. 1(c)). The resonances typically have a width of 5–10 MHz, and their Q-factor is thus 1000–2000. The dielectric constant of Si ($\epsilon_r = 11.9$) is high, explaining a significant shift in the resonant frequency upon mounting the silicon sample. The Q-factor is limited by the temperature and is expected to increase significantly below 4.2 K. Figure 1(d) shows a Smith Chart plot of the resonance curve corresponding to the upper trace (empty resonator) in Fig. 1(c). The Smith Chart reveals that our resonators are slightly undercoupled with a coupling coefficient estimated as $\kappa = 0.3$.

The exact orientation of the static magnetic field with respect to the thin film superconductor is critical, since a perpendicular field component of approximately 1 mT is sufficient to be threaded through the film. Trapped flux remains in the film, causing local field distortions and significant hysteretic frequency shifts of the resonance and a decrease in resonator Q-factor.[2] We reproducibly achieved satisfactory alignment by gradually increasing the external field from zero to its target value of 350 mT while compensating any frequency shifts and Q-factor reductions by carefully readjusting the orientation of the superconducting film. Whenever the misorientation was too large and flux was trapped, the superconductor was annealed by raising its temperature above the transition temperature. High-Q resonances have been observed up to fields of 1 T.

Pulsed ESR experiments are performed using a commercial X-band spectrometer (Bruker ElexSys 580). A Hahn echo sequence with two refocussing pulses $[\pi/2(+x) - \tau - \pi(+y) - \tau - \text{echo1} - \tau - \pi(+y) - \tau - \text{echo2}]$ is employed to measure T_2 of P donors. T_1 of donors is longer than 10 s at 4.2 K (Ref. 14). In order to allow faster acquisition time not limited by T_1, we illuminated the sample with an infrared light emitting diode for 100 ms followed by a delay of 50 ms to thermalize the spins before running the echo pulse sequence. Figure 2(a) illustrates a typical time-domain transient with two echo signals after 1000 signal averaging

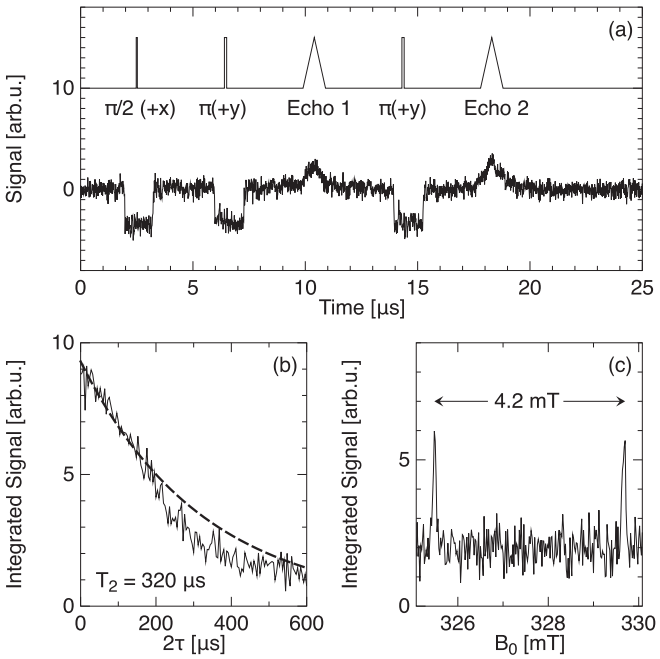

FIG. 2. (a) Hahn echo signals (bottom trace) measured at 4.2 K with the pulse sequence shown at top. Two refocussed echoes are seen after two refocussing pulses. The $\pi/2$ and π pulses are 50 ns and 100 ns long, respectively. The pulses in the experimental trace appear broader than they are because of overlapping defense pulses. (b) Hahn echo decay as a function of 2τ (solid line), along with an exponential fit with time constant $T_2 = 320$ μs (dashed line). The decay curve does not follow the exponential for $2\tau > 200$ μs due to field fluctuations in the magnet (see Ref. 20). (c) An ESR spectrum measured by integrating the echo signal while sweeping the magnetic field. The two hyperfine split lines are 4.2 mT apart as expected for P donors.

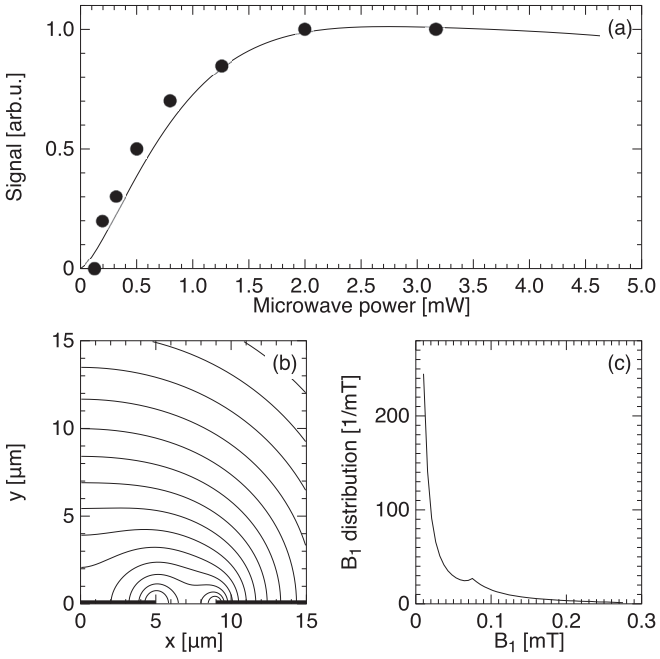

FIG. 3. (a) Microwave power dependence of the Hahn echo signal intensity (measured data: solid circles; simulation: line). (b) A contour plot of microwave magnetic field magnitude B_1 in one quadrant in the plane perpendicular to the CPW. The contour lines are spaced logarithmically with the field decreasing by 20% from one contour to the next. The location of center conductor and ground plane metallization are indicated as bold black lines. (c) Distribution of calculated B_1 values at applied microwave power of 2 mW.

accumulations. The second echo is stronger because the rotation errors of the pulses are partially cancelled after the second π pulse. The echo amplitude decays exponentially with 2τ and is a direct measure of T_2 (Fig. 2(b)). From the fit we establish $T_2 = 320$ μs, in excellent agreement with previous measurements.[13] In the field sweep experiment in Fig. 2(c) the delay time τ is kept constant, whereas the external field is scanned. The two hyperfine lines split by 4.2 mT are resolved providing a definite signature of P donors. The echoes shown in Fig. 2(a) have a FWHM of approximately 1 μs. This corresponds to a linewidth of 0.01 mT, close to the value established for this sample in previous measurements. This means that the superconducting layer does not distort the homogeneity of the static magnetic field substantially. The microwave pulse power used in these experiments was $P = 2$ mW, four orders of magnitude lower than for a waveguide resonator (Bruker MD5 dielectric resonator resonator with $Q \approx 1500$) in an equivalent experiment.[13]

III. DISCUSSION

A. Modeling

The distribution of B_1 fields in the plane perpendicular to the CPW is determined by the characteristic geometry of the CPW signal and ground plane lines, the dielectric constant above and below the waveguide, and the sample thickness. Figure 3(b) shows the B_1 magnitude for our particular geometry, calculated using a conformal mapping technique.[15] B_1 is inhomogeneous across the sample volume, reaching its maximum in the gap between signal and ground lines and decreasing rapidly towards the sample interior.

The rotation angle θ of a rectangular pulse of strength B_1 and duration t_p is given by

$$\theta = g\mu_B B_1 t_p/\hbar, \tag{1}$$

where g is the electron g-factor and μ_B is the Bohr magneton. Because of the broad B_1 distribution only a fraction of the spins experience the desired rotation θ, whereas all other spins are either over or under rotated. In waveguide resonators that have a narrow B_1 distribution (e.g., less than 10%),[16] the echo amplitude after applying the Hahn echo sequence $[\theta_1 - \tau - \theta_2 - \tau - \text{echo}]$ with $\theta_2 = 2\theta_1$ varies as $\sin^3\theta_1$, exhibiting pronounced oscillations of the echo amplitude as a function of B_1 with maxima at $\theta_1 = k\pi/2$ and $\theta_2 = k\pi$, where k is odd. In comparison, because of the broad B_1 distribution such oscillations are not seen in the power dependence measured in our CPW resonators (Fig. 3(a)). Instead, the dependence is barely peaked, reaching the maximum intensity at microwave power around 2 mW and remaining flat at higher powers.

We simulated the power dependence in Fig. 3(a) by summing up the contributions of all spins and taking into account the field strength $B_1\boldsymbol{r}$ at each spin location $\boldsymbol{r}$,[17]

$$\text{signal}\,(P) = A \int d\boldsymbol{r}\, \sin^3\theta\,(P, \boldsymbol{r})\, g_S\,(\boldsymbol{r})\, \rho, \tag{2}$$

where ρ is the donor spin density, P is the applied microwave power, and A is an amplitude scaling factor. This expression

differs from the one commonly found in the ESR literature by the presence of an additional factor $g_S(\boldsymbol{r})$, the spin-to-resonator coupling constant.[9,10] In our case, the B_1 field in the CPW resonator is highly inhomogeneous and therefore $g_S(\boldsymbol{r})$ varies substantially depending on the location of the spin with respect to the CPW. According to the *principle of reciprocity* derived by Hoult and Bhakar,[17] $g_S(\boldsymbol{r})$ is proportional to the $B_1'(\boldsymbol{r})$ field seen by a spin at a location $\boldsymbol{r}$ in the ground state of the resonator. For fitting purposes, Eq. (2) can be rewritten in the form

$$\text{signal}\,(P) = A' \int d\boldsymbol{r}\, \sin^3\theta\,(P, \boldsymbol{r})\, B_1'(\boldsymbol{r})\rho, \qquad (3)$$

where we substituted g_S for B_1', and all constant parameters entered the new scaling factor A'. The rotation angle $\theta(P, \boldsymbol{r})$ is calculated according to Eq. (1) with the magnetic field $B_1(P, \boldsymbol{r}) = C\sqrt{P}B_1'(\boldsymbol{r})$ being a function of applied microwave power P and spin location $\boldsymbol{r}$. Our model thus has only three fitting parameters: the microwave power to magnetic field conversion efficiency C, the amplitude scaling factor A', and the distance d_0 of the sample to the CWP metallization layer (Fig. 1(b)) that defines the integration (sample) volume in Eq. (3). All three can be established by fitting the model to the measured data (solid line in Fig. 3(a)). For example, the extracted d_0 is 5 μm, which is quite reasonable.

The extracted microwave conversion efficiency allows us to calculate the distribution of absolute B_1 fields at each applied microwave power. Figure 3(c) shows the calculated B_1 field distribution at 2 mW pulse power that corresponds to the power where the echo amplitude saturates as seen in Fig. 3(a)). The calculated distribution diverges at low B_1 fields because the number of contributing spins increases with distance from the waveguide. However, these remote spins do not contribute to the signal and our calculations show that the nearby spins within a lateral distance of 15 μm from the waveguide constitute 95% of the total echo signal.

B. Sensitivity

The resonator volume can thus be assumed to be $V = 30\,\mu\text{m} \times 10\,\mu\text{m} \times 3\,\text{mm}$ which gives a total number of spins of $N \approx 4.5 \times 10^9$ per hyperfine split line for the given doping concentration. The signal-to-noise ratio established from transient measurements (Fig. 2(a)), scaled to a single shot (no signal averaging) is approximately ~0.63, and ~10 when the echo signal is integrated over its width of 1 μs. This corresponds to a single shot sensitivity of 4.5×10^8 spins. This number is two orders of magnitude better than the sensitivity of a waveguide resonator under comparable conditions. We estimate that the sensitivity can be further improved by a factor of 2.5 if the sample is mounted closer to the resonator surface ($d_0 = 100$ nm instead of 5 μm). The sensitivity is expected to improve even further when the resonator is cooled down below 4.2 K, which would lead to significantly higher Q-factor.

Our spin number sensitivity compares favorably with those reported for other micro-resonator structures. Narkowicz, Suter, and Stonies[4] report a signal-to-noise ratio of 560 after 1000 acquisitions from 9.4×10^{14} spins using a lumped-element resonator with a coil diameter of 0.2 mm and a DPPH sample. Scaled to a sensitivity per shot, this corresponds to 3×10^{13} spins, which is five orders lower than in our case. Twig *et al.*[6] report a sensitivity of 1.5×10^6 spins/$\sqrt{\text{Hz}}$ from a CPMG sequence using a non-superconducting surface loop-gap resonator and a Si:P sample that is similar to ours. Their experiments are done at $T = 10$ K, where $T_1 \approx T_2$, allowing an effective acquisition rate of 100 kHz (100 CPMG echoes at a rate of 1 kHz). The sensitivity per shot is thus 4.8×10^8, quite comparable to our results.

IV. CONCLUSIONS

In conclusion, we have fabricated a thin film superconducting coplanar waveguide resonator and evaluated its performance with pulsed ESR spectroscopy on ^{28}Si:P epilayer samples. The small resonator volume and consequently its high filling factor leads to a high sensitivity, in particular towards spins close to the interface between resonator and sample. The peak power required for microwave pulses is in the mW range, which is compatible with low temperature operation. The superconducting layer does not introduce a significant distortion of the external magnetic field when the resonator is oriented parallel to the field. The inhomogeneous microwave field distribution leads to a complex dependence of echo intensity on microwave power which can be accurately described by model calculations taking the specific resonator geometry into account. This field inhomogeneity limits the fidelity of multi-pulse sequences, which should be partly resolved by using adiabatic pulses.[18,19] The resonator is a useful alternative to conventional waveguide resonators for studying small numbers of electron spins at or near a surface.

ACKNOWLEDGMENTS

This work was supported by the National Science Foundation (NSF) through the Princeton Materials Research Science and Engineering Center (DMR-0819860), the National Security Agency (NSA)/Laboratory for Physical Sciences through the Lawrence Berkley National Laboratory (LBNL) (100000080295), and the FWF (Vienna, Austria, J2903-N20).

[1] B. Johansson, S. Haraldson, L. Pettersson, and O. Beckman, Rev. Sci. Instrum. **45**, 1445 (1974).
[2] W. J. Wallace and R. H. Silsbee, Rev. Sci. Instrum. **62**, 1754 (1991).
[3] H. J. Mamin, R. Budakian, and D. Rugar, Rev. Sci. Instrum. **74**, 2749 (2003).
[4] R. Narkowicz, D. Suter, and R. Stonies, J. Magn. Reson. **175**, 275 (2005).
[5] R. Narkowicz, D. Suter, and I. Niemeyer, Rev. Sci. Instrum. **79**, 084702 (2008).
[6] Y. Twig, E. Dikarov, W. D. Hutchinson, and A. Blank, Rev. Sci. Instrum. **82**, 076105 (2011).
[7] A. C. Torrezan, T. P. Mayer Alegre, and G. Medeiros-Ribeiro, Rev. Sci. Instrum. **80**, 075111 (2009).
[8] J. H. Wesenberg, A. Ardavan, G. A. D. Briggs, J. J. L. Morton, R. J. Schoelkopf, D. I. Schuster, and K. Mølmer, Phys. Rev. Lett. **103**, 070502 (2009).
[9] D. I. Schuster, A. P. Sears, E. Ginossar, L. DiCarlo, L. Frunzio, J. J. L. Morton, H. Wu, G. A. D. Briggs, B. B. Buckley, D. D. Awschalom, and R. J. Schoelkopf, Phys. Rev. Lett. **105**, 140501 (2010).
[10] Y. Kubo, F. R. Ong, P. Bertet, D. Vion, V. Jacques, D. Zheng, A. Dréau, J.-F. Roch, A. Auffeves, F. Jelezko, J. Wrachtrup, M. F. Barthe, P. Bergonzo, and D. Esteve, Phys. Rev. Lett. **105**, 140502 (2010).

[11]Y. Kubo, C. Grezes, A. Dewes, T. Umeda, J. Isoya, H. Sumiya, N. Morishita, H. Abe, S. Onoda, T. Ohshima, V. Jacques, A. Dréau, J.-F. Roch, I. Diniz, A. Auffeves, D. Vion, D. Esteve, and P. Bertet, Phys. Rev. Lett. **107**, 220501 (2011).
[12]X. Zhu, S. Saito, A. Kemp, K. Kakuyanagi, S.-i. Karimoto, H. Nakano, W. J. Munro, Y. Tokura, M. S. Everitt, K. Nemoto, M. Kasu, N. Mizuochi, and K. Semba, Nature (London) **478**, 221 (2011).
[13]A. M. Tyryshkin, S. A. Lyon, A. V. Astashkin, and A. M. Raitsimring, Phys. Rev. B **68**, 193207 (2003).
[14]G. Feher and E. A. Gere, Phys. Rev. **114**, 1245 (1959).
[15]K. C. Gupta, R. Garg, and I. J. Bahl, *Microstrip Lines and Slotlines* (Artech House, 1979).
[16]J. J. L. Morton, A. M. Tyryshkin, A. Ardavan, K. Porfyrakis, S. A. Lyon, and G. A. D. Briggs, Phys. Rev. A **71**, 012332 (2005).
[17]D. I. Hoult and B. Bhakar, Concepts Magn. Reson. **9**, 277 (1997).
[18]J. Baum, R. Tycko, and A. Pines, Phys. Rev. A **32**, 3435 (1985).
[19]R. A. De Graaf and K. Nicolay, Concepts Magn. Reson. **9**, 247 (1997).
[20]A. M. Tyryshkin, J. J. L. Morton, S. C. Benjamin, A. Ardavan, G. A. D. Briggs, J. Ager, and S. A. Lyon, J. Phys.: Condens. Matter **18**, S783 (2006).